Atomic Spectroscopy

Article

Quasi-Non-Destructive Multi-Element Characterization of Polymer Materials for 3D-Printed Firearms by Liquid Microjunction Sampling into Inductively Coupled Plasma Mass Spectrometry (LMJ-ICPMS)

Jordan Chiabai and Diane Beauchemin *

Queen's University, Department of Chemistry, 90 Bader Lane, Kingston, ON K7L 3N6, Canada

Received: *July 19, 2026;* ***Revised:*** *August 10, 2026;* ***Accepted:*** *August 11, 2026;* ***Available online:*** *August 11, 2026.*

DOI: 10.46770/AS.2026.0061

ABSTRACT: In this proof-of-concept study, liquid microjunction inductively coupled plasma mass spectrometry (LMJ-ICPMS) was used as a localized, quasi-non-destructive approach for the qualitative trace elemental characterization of polymer materials relevant to forensic investigations involving 3 dimensions (3D)-printed firearms. Blue nylon glass-fibre-reinforced polyamide 6 (PA6-GF), polyethylene terephthalate glycol (PETG), and polylactic acid (PLA) were analyzed using a custom LMJ sampling interface coupled to quadrupole-based ICPMS. Measurable transient signals were obtained for multiple elements directly from polymer surfaces, demonstrating the capability of LMJ sampling to recover and transport trace elemental constituents with minimal sample preparation and limited surface disruption. Distinct normalized elemental profiles were observed between PA6-GF and PETG, with PETG exhibiting higher relative abundances of Mg, Ca, Ti, and Sr, whereas PA6-GF exhibited elevated Ba. Complete separation between PA6-GF and PETG was achieved using Ti/Mg and Ba/Ca elemental ratios, while targeted and untargeted principal component analyses demonstrated distinct clustering based on selected elemental markers and the broader elemental profile, respectively. The first two principal components of the targeted analysis accounted for 97.7% of the total variance. Addition of 2% (v/v) methanol (MeOH) to the 2% (v/v) nitric acid (HNO_3) sampling solvent improved elemental recovery of PLA, enabling multivariate differentiation of PA6-GF, PETG, and PLA, with the first two principal components accounting for 97.0% of the total variance. These results demonstrate the applicability of LMJ-ICPMS for qualitative elemental profiling and differentiation of polymer materials, while highlighting the importance of solvent optimization for extending the approach to chemically distinct polymer systems.

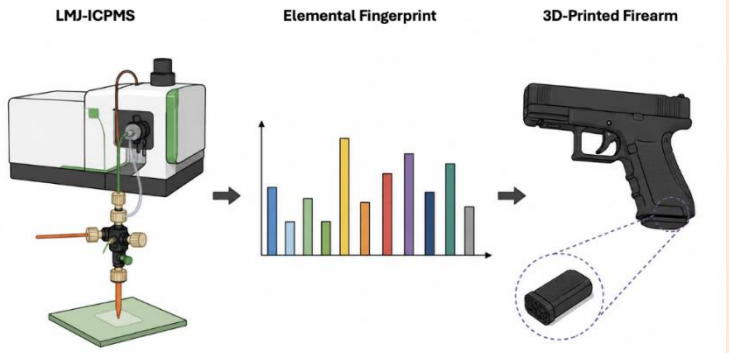

INTRODUCTION

Recent law enforcement operations in Canada underscore the growing significance of three dimensions (3D)-printed firearms ("ghost guns"), with a nationwide operation resulting in the seizure of approximately 440 conventional and 3D-printed firearms and 52 3D printers used in their manufacture.[1] Thermoplastic polymers such as nylon glass-fibre-reinforced polyamide 6 (PA6-GF), polyethylene terephthalate glycol (PETG), and polylactic acid (PLA) are widely used in additive manufacturing applications due to their accessibility and tunable mechanical properties.[2-4] These materials often contain a range of additives, including pigments, fillers, and stabilizers, which contribute to differences in their elemental composition and can vary significantly between

manufacturers and formulations.

In forensic contexts, previous studies have demonstrated that polymer residues can be transferred onto bullets, cartridge cases, and surrounding surfaces during use.[2, 3, 5] However, the abundance and detectability of these residues are often low and highly variable, limiting their practical utility without sensitive analytical methods. The ability to differentiate polymer materials based on their chemical composition may provide associative evidence linking recovered residues, fragments, or manufactured components to a common source. Furthermore, whereas spectroscopic techniques can differentiate polymer classes, discrimination between visually similar materials, particularly black polymers, remains limited.[3, 4] In addition, polymer substrates may produce inconsistent or incomplete toolmarks, reducing the reliability of conventional microscopic comparison methods.[3, 5, 6]

A variety of analytical techniques have been investigated for the characterization of polymer materials associated with 3D-printed firearms. Microscopic examination has been used to evaluate the morphology and distribution of polymer residues recovered following firing events; however, these methods provide limited chemical information and are often insufficient for source discrimination.[5] Vibrational spectroscopy techniques, including Fourier transform infrared and Raman spectroscopies, have demonstrated utility for differentiating common filament materials, but their application to trace-level residues and highly pigmented materials may be limited by weak signal intensity, fluorescence interference, and signal suppression associated with carbon black-containing formulations.[3]

Ambient mass spectrometry techniques, such as direct analysis in real time (DART-MS), enable rapid analysis of polymer-derived compounds and additives with minimal sample preparation and have been applied to polymer residues associated with 3D-printed firearms.[2, 7] However, discrimination among chemically similar materials may remain challenging because polymer formulations often share common molecular components and additives. More comprehensive compositional information can be obtained using bulk techniques, such as pyrolysis gas chromatography-mass spectrometry; however, these approaches are inherently destructive and require the removal of material from the sample.

Elemental analysis provides an alternative approach for polymer characterization by targeting inorganic constituents associated with pigments, fillers, catalysts, and other manufacturing additives. As these components can vary among polymer formulations, elemental signatures may provide discriminatory information beyond that obtained from molecular characterization alone. Laser-induced breakdown spectroscopy (LIBS) has been successfully applied to the identification and differentiation of polymer materials based on their elemental composition.[8] Although LIBS enables rapid elemental characterization with minimal sample preparation, its performance can be influenced by matrix effects arising from the strong dependence of the sampling and plasma formation processes on the sample matrix.[9] Laser ablation inductively coupled plasma mass spectrometry (LA-ICPMS) enables spatially resolved elemental profiling and has demonstrated the ability to differentiate polymer materials, including visually similar black polymers.[10] However, LA-ICPMS is inherently destructive because elemental information is obtained through laser ablation of the sample surface and may be affected by matrix-dependent effects and variability in ablation behavior, which can limit reproducibility for heterogeneous substrates.[10]

Conventional solution-based ICPMS is widely used for trace elemental analysis because of its high sensitivity and multi-element detection capability.[11] Within forensic science, ICPMS has been applied to the elemental characterization of evidentiary materials, where trace elemental profiles can provide valuable discriminatory information for source comparison.[12] However, conventional solution-based ICPMS typically requires bulk sample digestion, which consumes the sample, eliminates spatial information, and may limit the availability of evidence for subsequent or complementary analyses.[11] To get around these limitations, Manard and co-workers modified the Plate Express device (from Advion Interchim Scientific) that was developed for extracting analytes from thin layer chromatography plates to directly sample particles from surfaces for single particle ICPMS while preserving spatial information.[13] However, the approach has not been used for forensic applications.

A significantly cheaper approach is liquid microjunction (LMJ) surface sampling, which was originally developed by Van Berkel and co-workers as a localized surface sampling technique in MS.[14] LMJ has been adapted for a range of analytical applications and comprehensively reviewed by Simon and Oleschuk.[15] When coupled with ICPMS, LMJ offers a promising approach for localized, quasi-non-destructive elemental analysis by enabling controlled extraction of analytes through the formation of a confined liquid junction at the sample surface with minimal disruption.[15] A proof-of-concept study demonstrated the feasibility of LMJ-ICPMS for localized elemental analysis of solid substrates,[16] but primarily focused on homogeneous materials and inorganic systems. As a result, the performance of LMJ-ICPMS for chemically heterogeneous polymer materials, particularly at trace levels, remains unexplored. Yet, LMJ-ICPMS is particularly attractive for forensic polymer characterization, as it combines localized elemental analysis with minimal sample preparation and limited surface disruption, while preserving most of the evidence for subsequent analysis. These characteristics are also consistent with principles of green analytical chemistry, as direct analysis reduces waste, energy consumption, and hazardous reagents while maintaining analytical performance.[17]

For the first time, this work evaluates the application of LMJ-ICPMS as a localized, quasi-non-destructive approach for the qualitative trace elemental characterization of polymer materials. To this end, the approach is applied to PA6-GF, PETG, and PLA to evaluate its ability to characterize polymer materials and differentiate materials based on their elemental signatures using qualitative elemental profiling. The influence of sampling solvent composition on analyte recovery is also investigated. The expectation was that chemically different polymer materials would produce distinct elemental profiles, enabling their differentiation based on qualitative elemental composition.

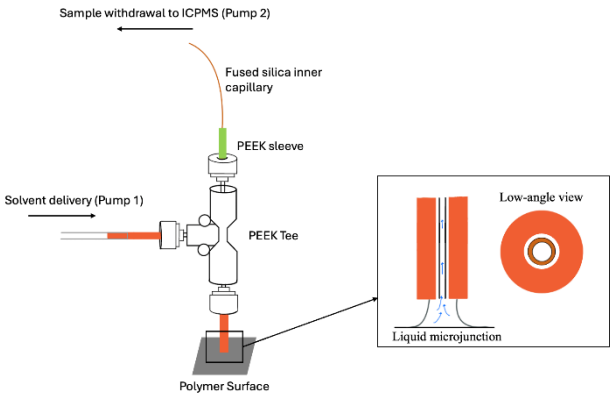

Fig. 1 Schematic representation of the LMJ sampling interface used for localized elemental analysis of polymer samples. The inset illustrates the formation of the LMJ at the polymer surface.

EXPERIMENTAL

Samples. Polymer samples consisted of 3D-printed thermoplastics fabricated from commercially available filaments (Bambu Lab, Shenzhen, China). Materials analyzed included blue nylon PA6-GF, PETG in multiple colors (white, green, blue, and yellow), and white PLA. All samples were fabricated using a Bambu Lab H2C 3D printer (Bambu Lab, Shenzhen, China) as flat, square substrates. No surface pre-treatment or cleaning procedures were performed prior to analysis to avoid potential removal or redistribution of surface-associated material.

LMJ-ICPMS instrumentation. Trace elemental analysis was performed using a NexION 2000 quadrupole-based ICPMS instrument (PerkinElmer, Waltham, MA, USA) equipped with a high-sensitivity glass cyclonic spray chamber with a matrix gas port (PerkinElmer, Waltham, MA, USA), a Burgener Teflon Mira Mist TMM-3500 nebulizer (Burgener Research Inc., Mississauga, ON, Canada), and a custom LMJ sampling interface. The LMJ probe (Fig. 1) was constructed based on previously reported designs,[15] using a polyetheretherketone (PEEK) tee (508 µm I.D. × 1599 µm O.D.) housing concentric PEEK tubing. A fused silica inner capillary (200 ± 10 µm I.D. × 360 ± 10 µm O.D.) was positioned within the assembly to transport extracted analyte solution directly to the ICPMS nebulizer. The probe design incorporated an external PEEK sleeve to improve mechanical stability and facilitate consistent LMJ formation at the sample surface.

LMJ sampling procedure. LMJ sampling was performed under continuous flow conditions using two independently controlled peristaltic pumps. The first peristaltic pump delivered fresh sampling solvent to the LMJ probe at a flow rate of 63-68 µL min^{-1} to establish and maintain a stable LMJ at the sample surface. A second peristaltic pump withdrew the solvent containing the extracted analytes from the LMJ and transported it directly to the ICPMS nebulizer at approximately 192 µL min^{-1}. Independent control of the solvent delivery and withdrawal flow rates was required to maintain a stable LMJ. The sampling solvent consisted of 2% (v/v) HNO_3 prepared from sub-boiled HNO_3 (ACS grade; Fisher Scientific, Ottawa, ON, Canada) purified in-house using a sub-boiling distillation system (Savillex, Minnetonka, MN, USA) and diluted with doubly deionized water (DDW, 18.2 MΩ cm) produced using an Arium Pro UV/DI system (Sartorius Stedim Biotech, Göttingen, Germany). This solvent was used for PETG and PA6-GF samples. For PLA samples, both 2% (v/v) HNO_3 and a mixture of 2% (v/v) HNO_3 + 2% (v/v) MeOH (HPLC grade; Sigma-Aldrich, Saint Louis, MO, USA) were evaluated to assess extraction performance.

Table 1. Operating conditions of LMJ-ICPMS

Parameter	Setting
RF Power (W)	1600
Ar plasma gas flow rate (L min^{-1})	18
Ar auxiliary gas flow rate (L min^{-1})	1.2
Ar nebulizer gas flow (L min^{-1})	0.92
Dwell time (ms amu^{-1})	50
Detector mode	Dual (pulse/analog)
Acquisition mode	Transient

The LMJ was formed by bringing the probe into contact with the polymer surface, enabling localized extraction of surface-accessible analytes (inset of Fig. 1). The probe remained stationary during sampling and was maintained in contact with the sample surface for approximately 1 min. Replicate measurements were collected from multiple locations across each sample surface to assess measurement reproducibility and spatial variability.

ICPMS operating conditions. The operating conditions are summarized in Table 1. The instrument was tuned prior to analysis using a 1 µg L^{-1} multi-element tuning solution to optimize sensitivity, mass calibration, and doubly charged ion production. The dynamic reaction cell was not used during analysis. A broad suite of elements was monitored, including Mg, Al, Ca, Sc, Ti, V, Cr, Mn, Fe, Co, Ni, Cu, Zn, Ga, Rb, Sr, Nb, Ru, Rh, Pd, Ag, Cd, In, Sn, Sb, Ba, Hg, and Pb. Data acquisition parameters, including

dwell times, were optimized using instrument default methods for multi-element screening.

Data processing and analysis. Time-resolved signals were processed in Microsoft Excel using manual baseline correction. Baseline regions were selected from stable portions of the signal preceding analyte extraction. Baseline-corrected transient signals were obtained by subtracting the average baseline intensity from each individual data point across the LMJ peak. Blank measurements of the sampling solvent were made periodically throughout the study to confirm that the baseline signal remained consistent and that there was no significant contamination. Net signal intensities were determined by integration of the baseline corrected transient signal over the duration of the LMJ peak, defined from the onset of the transient response until the signal returned to baseline. Between 5 and 16 replicate measurements were collected depending on sample type and experimental objective. Potential outliers were evaluated using Grubbs' test at the 95% confidence level prior to statistical analysis.

To facilitate comparison between samples, elemental responses were subjected to sum normalization across the selected elements. For each measurement, the signal intensity of each element was divided by the sum of the signal intensities of all selected elements, resulting in relative contribution of each element to the total measured elemental signal. This approach minimizes variations in overall signal intensity and enables comparison of the relative elemental composition among samples. Elemental ratios were subsequently calculated for selected element pairs to evaluate their utility for material discrimination. Principal component analysis (PCA) was performed using normalized elemental data to assess multivariate differences between polymer materials. Differences among polymer groups were evaluated using one-way analysis of variance (ANOVA) followed by Tukey post hoc testing, with statistical significance defined as $p < 0.05$. No external calibration was performed due to the absence of suitable matrix-matched reference materials. Consequently, results are reported in terms of relative signal intensity, sum-normalized elemental abundance, and elemental ratios rather than absolute elemental concentrations.

Multi-element detection from polymer surfaces. Time-resolved LMJ-ICPMS analysis produced measurable transient signals for multiple elements detected on blue PA6-GF and PETG surfaces using 2% (v/v) HNO_3 as the leaching solution. Representative transient responses are shown in Fig. 2; similar signal profiles were observed for the remaining detected elements monitored throughout the study, indicating consistent extraction and transport through the LMJ interface. To obtain these profiles, data acquisition was initiated and the LMJ probe was put in contact with the sample surface and maintained on the same spot until the analyte signal returned to baseline. The well-defined transient profiles obtained for multiple elements, which are similar to those previously reported by LMJ-ICPMS for a dried up aliquot of

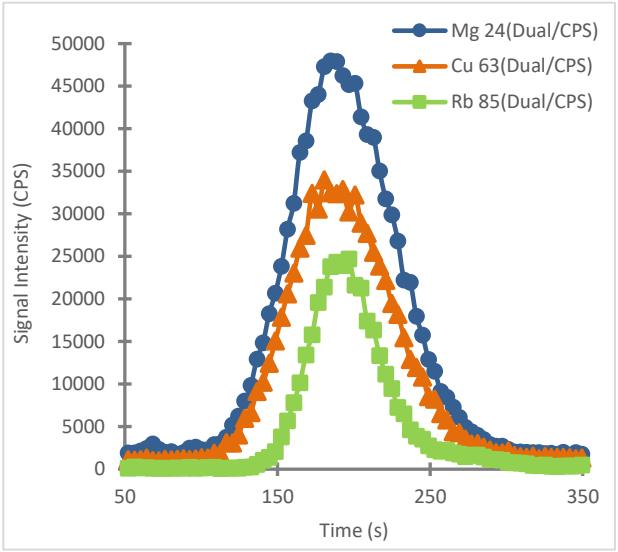

Fig. 2 Representative multi-element transient signal obtained from LMJ-ICPMS analysis of a blue PA6-GF sample.

standard solution,[16] demonstrate that LMJ sampling provides a reliable means of extracting and introducing analytes into ICPMS for elemental characterization.

Similar normalized elemental profiles were obtained from multiple LMJ sampling locations on the same white PETG sample (Fig. S1), indicating limited spatial variation in elemental composition at the scale investigated and good reproducibility of the elemental profile. These sum-normalized results provide the basis for subsequent comparison of elemental profiles between polymer materials. Sum normalization was required to compensate for variations in extraction efficiencies or surface heterogeneity, which can be inferred from the significant differences in analyte signal intensities measured at different locations on the sample (Fig. S2). As only one sample of each polymer produced from filaments obtained from a single manufacturer was analyzed, assessing between-sample variability will be the subject of future work. The extent to which the observed elemental signatures are representative of other manufacturers, production batches, or polymer formulations will also be the subject of a future study. Indeed, the robustness of the sum-normalization approach remains to be demonstrated for other polymers, as it may not compensate for matrix-dependent extraction effects, where extraction efficiency is analyte dependent.

Polymer differentiation based on qualitative elemental composition. Mean sum-normalized elemental profiles obtained from replicate LMJ extractions collected from multiple locations across each polymer sample for blue PA6-GF and four PETG color variants are shown in Fig. 3. Clear differences in elemental composition were observed between the two polymer types.

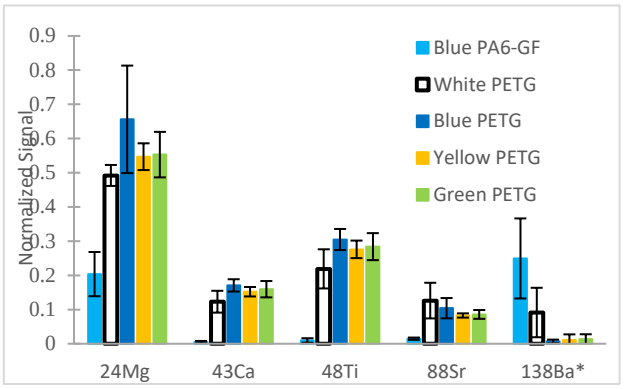

Fig. 3 Comparison of the mean sum-normalized relative abundances of the selected discriminatory elements (Mg, Ca, Ti, Sr, and Ba) for blue PA6-GF and PETG color variants (n = 15 for blue PA6-GF and white PETG; n = 5 for blue, green, and yellow PETG). Error bars represent one standard deviation. *PETG ^{138}Ba values were multiplied by 15 for visualization purposes only.

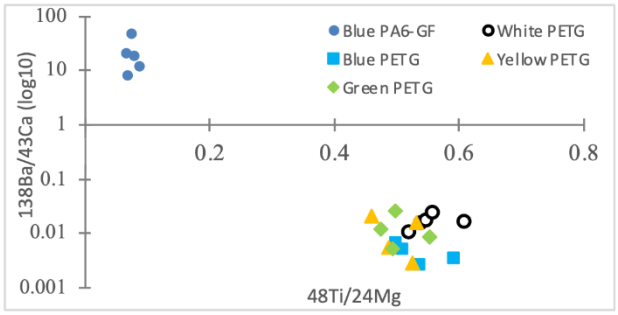

Fig. 4 Separation of blue PA6-GF and PETG variants using Ti/Mg and Ba/Ca elemental ratios (n = 5).

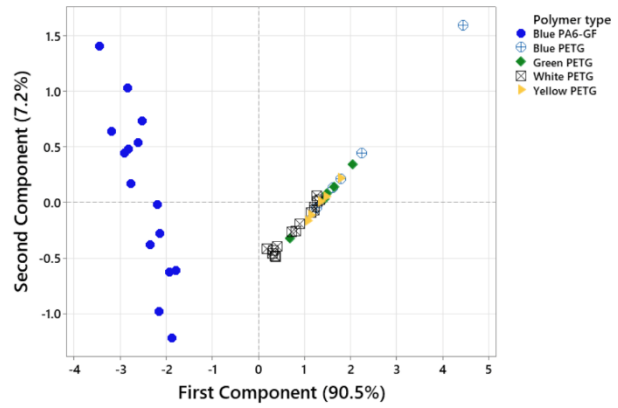

Fig. 5 Targeted PCA score plot of sum-normalized data for Mg, Ca, Ti, and Ba showing separation of blue PA6-GF and PETG variants using 2% (v/v) HNO_3.

PETG samples exhibited higher relative abundances of Mg, Ca, Ti, Sr, whereas blue PA6-GF exhibited a substantially greater relative abundance of Ba. These trends were observed consistently across all PETG color variants. One-way ANOVA followed by Tukey post hoc testing confirmed significant differences ($p < 0.05$) between PA6-GF and all color variants for Mg, Ca, Ti, Sr, and Ba. Among the PETG color variants, blue PETG exhibited significantly greater normalized abundances of Mg, Ca, and Ti than white PETG, whereas green and yellow PETG displayed intermediate abundances and were not significantly different from either blue or white PETG. No significant differences were observed among the PETG color variants for Sr or Ba. These results indicate that the elemental signatures obtained by LMJ-ICPMS are primarily influenced by polymer type rather than filament color.

Although differences among the PETG color variants were observed for Mg, Ca, and Ti, the overall similarity of their elemental profiles is notable. Despite differences in pigmentation, the PETG samples exhibited consistent relative abundances of Mg, Ca, Ti, and Sr, suggesting the presence of a reproducible elemental profile characteristic of the PETG materials examined. In contrast, blue PA6-GF exhibited a distinct elemental signature characterized by elevated Ba abundance. The observation that polymer type produced greater differences in elemental composition than filament color suggests that LMJ-ICPMS captures information associated with the underlying material formulation.

Elemental ratio-based differentiation. To further evaluate the discriminatory capability of LMJ-ICPMS, elemental ratios were examined as compositional markers for polymer differentiation. Several elemental ratio combinations were evaluated, and the Ti/Mg and Ba/Ca ratios provided the greatest separation between the polymer types (Fig. 4). Complete separation was observed between blue PA6-GF and all PETG variants, with no overlap between the two polymer types. Blue PA6-GF samples clustered at low Ti/Mg ratios and high Ba/Ca ratios, whereas the PETG samples clustered at high Ti/Mg and low Ba/Ca ratios. The distinct grouping observed for each material reflects the elevated relative abundance of Ti in PETG and Ba in PA6-GF, consistent with the elemental profiles in Fig. 3.

The strong separation achieved using only two elemental ratios indicates that the compositional differences between PA6-GF and PETG are systematic and reproducible. The ability to achieve complete separation using a limited number of elemental markers suggests that a relatively simple ratio-based approach may be sufficient for polymer differentiation in some applications. However, because the ratios were selected based on elements that exhibited strong discriminatory power, this approach represents a targeted assessment of compositional differences between materials.

Targeted multivariate analysis of polymer materials. To further evaluate the observed separation, PCA was performed using the four elemental markers (Mg, Ca, Ti, and Ba) identified from the elemental ratio analysis. The resulting PCA score plot is shown in Fig. 5. Clear separation was observed between the blue PA6-GF

and PETG color variants, with no overlap between the two material groups. Separation occurred primarily along the first principal component (PC1), which accounted for 90.5% of the total variance, while the second principal component (PC2) accounted for an additional 7.2%, resulting in a cumulative variance of 97.7%.

The targeted PCA produced separation consistent with the elemental ratio analysis, demonstrating that the four selected elemental markers effectively capture the compositional differences between PA6-GF and PETG. Although minor variation was observed among the PETG color variants, substantial overlap between the four colors indicates that polymer type had a greater influence on the elemental profiles than filament color. The high cumulative variance explained by the first two principal components indicates that these four elements contain most of the discriminatory information required for polymer classification.

Untargeted multivariate analysis of polymer materials. To determine whether the separation observed using the selected elemental markers was reflected across the broader elemental profile, PCA was performed using the complete sum-normalized elemental dataset to evaluate differences in the overall elemental profiles of the blue PA6-GF and PETG samples. The resulting PCA score plot (Fig. S3) shows a similar separation between the two polymer types, with no overlap between the blue PA6-GF and PETG clusters. Separation occurred primarily along PC1, which accounted for 34.6% of the total variance, while PC2 accounted for an additional 9.9%, resulting in a cumulative variance of 44.5%.

The untargeted PCA confirmed the trends observed using the targeted multivariate analysis, further demonstrating that blue PA6-GF and PETG possess distinct elemental signatures. Whereas the targeted PCA relied on four selected elemental markers, the untargeted PCA incorporated the broader elemental profile and therefore provided a more comprehensive assessment of sample similarity. The clear clustering observed in Fig. S3 indicates that the differences between PA6-GF and PETG are not limited to a small number of individual elements but are reflected across the broader elemental profile.

Additional multivariate and elemental ratio analyses were also evaluated for discrimination of the PETG color variants. PCAs incorporating Pb (Fig. S4), as well as Mn, Cu, and Sr (Fig. S5), together with 3D elemental ratio plots using combinations of Mg, Ca, Ti, Ba, and Pb (Figs. S6- S7) consistently distinguished PA6-GF from PETG. However, substantial overlap remained among the PETG color variants, indicating that reliable color discrimination could not be achieved under the present experimental conditions.

Preliminary evaluation of PLA extraction. Initial LMJ-ICPMS analysis of white PLA using 2% (v/v) HNO_3 as the sampling solvent produced minimal elemental response (Fig. S8). To improve analyte recovery, a modified sampling solvent consisting of 2% (v/v) HNO_3 and 2% (v/v) methanol (MeOH) was evaluated. The addition of MeOH resulted in a substantial increase in signal intensity relative to 2% (v/v) HNO_3 alone (Fig. S8), demonstrating improved extraction performance for PLA. Although the mechanism responsible for the improved extraction was not investigated, the results suggest that the addition of MeOH promoted more effective interaction between the sampling solvent and PLA surface, potentially improving surface wetting, and recovery of elemental constituents. These findings highlight the importance of solvent selection for LMJ-ICPMS analysis and suggest that polymer-specific solvent optimization may be required when extending the technique to chemically distinct polymer materials.

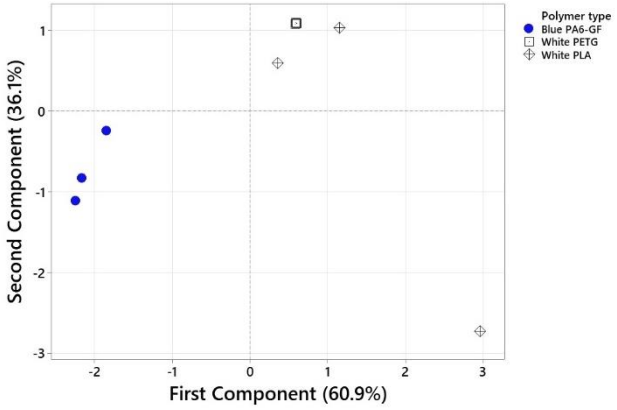

Fig. 6 Targeted PCA score plot of sum-normalized data for Mg, Ca, Ti, and Ba showing separation of PA6-GF, PETG, and PLA samples using 2% (v/v) HNO_3 + 2% (v/v) MeOH.

Effect of sampling solvent on polymer differentiation. Because the addition of MeOH enabled measurable elemental response from white PLA, PCA using the four elemental markers employed in the targeted multivariate analysis was performed to evaluate whether the modified sampling solvent could differentiate PA6-GF, PETG, and PLA based on their elemental profiles (Fig. 6). The PC1 accounted for 60.9% of the total variance, while the PC2 accounted for an additional 36.1%, resulting in a cumulative variance of 97.0%. The PCA showed distinct clustering of the polymer materials, with PETG forming a distinct cluster and greater variability observed among the PA6-GF and PLA measurements. The increased dispersion of the PLA data suggests that, although the addition of MeOH substantially improved analyte recovery, further optimization of the sampling conditions is required to improve measurement reproducibility.

CONCLUSION

For the first time, LMJ-ICPMS was used as a localized, quasi-non-destructive approach for the qualitative multi-element characterization of polymer materials relevant to 3D-printed firearm production. Time-resolved analysis produced measurable transient signals for multiple elements directly from polymer surfaces, demonstrating that LMJ sampling can recover and transport trace elemental constituents for ICPMS detection with minimal sample preparation and limited surface disruption.

Distinct elemental profiles were obtained for PA6-GF and PETG materials. PETG exhibited consistently higher relative abundances of Mg, Ca, Ti, and Sr, whereas PA6-GF exhibited elevated Ba. Statistical analysis confirmed significant differences between the PA6-GF and all PETG color variants for these elemental markers. Although subtle differences among the PETG color variants were observed for Mg, Ca, and Ti, the elemental signatures obtained by LMJ-ICPMS were primarily influenced by polymer type rather than filament color.

Elemental ratio analysis and multivariate statistical analysis provided complementary approaches for polymer discrimination. Complete separation between PA6-GF and PETG was achieved using the Ti/Mg and Ba/Ca ratios. Targeted PCA performed using Mg, Ca, Ti, and Ba accounted for 97.7% of the total variance, demonstrating that a limited number of elemental markers effectively captured the compositional differences between the polymer materials. Untargeted PCA performed using the broader elemental profile likewise produced clear separation between PA6-GF and PETG, confirming that the observed differences extended beyond a small subset of elements and were reflected throughout the overall elemental profiles.

The addition of 2% (v/v) MeOH to the sampling solvent improved elemental recovery from PLA, enabling measurable elemental responses that were not observed using the 2% (v/v) HNO_3 alone. The modified sampling solvent further enabled multivariate differentiation of PA6-GF, PETG, and PLA, demonstrating that solvent optimization can expand the applicability of LMJ-ICPMS to chemically distinct polymer materials. Although additional optimization is required to improve the reproducibility of PLA measurements, these findings highlight the importance of solvent composition for polymer-specific analysis.

Overall, this work demonstrates the applicability of LMJ-ICPMS for qualitative elemental profiling and discrimination of polymer materials associated with 3D-printed firearms. The ability to generate localized elemental fingerprints with minimal surface disruption provides a foundation for further evaluation of LMJ-ICPMS for the characterization and comparison of polymer evidence encountered in forensic investigations.

Future works should focus on optimizing the LMJ sampling conditions for PLA and other chemically distinct polymers through systematic evaluation of solvent composition and extraction parameters to improve analyte recovery and measurement reproducibility. Additional studies should expand the range of polymer materials examined to include independently manufactured samples from different polymer types, filament manufacturers, production batches, printer platforms, and color variants. Particular emphasis should be placed on black polymer materials, which are commonly encountered in 3D-printed firearm applications and remain difficult to differentiate using conventional analytical techniques. Investigation of a broader range of polymer formulations will provide a more comprehensive assessment of the robustness, reproducibility, and forensic utility of LMJ-ICPMS for the characterization and discrimination of polymer evidence.

ASSOCIATED CONTENT

The supporting information (Figs. S1-S8) is available at https://www.at-spectrosc.com

AUTHOR INFORMATION

Diane Beauchemin received her Ph.D. in 1984 from Université de Montréal. She is a professor (Full) at Queen's University. Her research efforts are focused on inductively coupled plasma mass spectrometry (ICPMS) and ICP optical emission spectrometry (OES) from both fundamental and application perspectives and expanding the range of application of ICPMS/OES to geochemical exploration, risk assessment of food safety, characterization of nanoparticles, and forensic analysis. Diane Beauchemin won the Alan Date Memorial Award (1988) from VG Elemental, the Distinguished Service Award (2001) from Spectroscopy Society of Canada, the Maxxam Award (2017) and Clara Benson Award (2019) from Canadian Society for Chemistry, the Gerhard Herzberg Award (2018) from the Canadian Society for Analytical Sciences and Spectroscopy, and the Environment Division Research and Development Dima Award from the Chemical Institute of Canada (2024). She is author or co-author of over 192 articles published in peer-reviewed scientific journals.

Corresponding Author

* D. Beauchemin

Email address: diane.beauchemin@queensu.ca

Notes

The authors declare no competing financial interest.

ACKNOWLEDGMENTS

The authors gratefully acknowledge the financial support of the Natural Sciences and Engineering Research Council of Canada (RGPIN-2024-06613). JC also thanks Queen's School of Graduate Studies for a Queen's graduate award, Darrian Prendergast for assistance with generating the PCA figures and the members of the Beauchemin Research Group for their valuable support and discussions throughout this work.

REFERENCES

1. Public Safety Canada. *Parliamentary Committee Notes: Ghost Guns and Illegal Manufacturing in Canada.* 2023. https://www.publicsafety.gc.ca/cnt/trnsprnc/brfng-mtrls/prlmntry-bndrs/20240220/13-en.aspx (accessed July 12, 2026)
2. O. Mahapatra and I. Jain, *J. Forensic Sci. Res.*, 2025, **9**, 173-178. https://doi.org/10.29328/journal.jfsr.1001098
3. M. S. Falardeau, C. Mireault, B. Daoust, and C. Muehlethaler, *Forensic Sci. Int.*, 2024, **357**, 111999. https://doi.org/10.1016/j.forsciint.2024.111999
4. M. V. Adamos, K. Pitts, S. W. Lewis, and G. Sauzier, *Forensic Chem.*, 2026, **48**, 100727. https://doi.org/10.1016/j.forc.2026.100727
5. T. Trincat, M. Saner, S. Schaufelbühl, M. Gorka, D. Rhumorbarbe, A. Gallusser, O. Delémont, and D. Werner, *Forensic Sci. Int.*, 2022, **331**, 111144. https://doi.org/10.1016/j.forsciint.2021.111144
6. Z. E. Wenzinger, S. Wetzel, B. Bernarding, J. Viator, B. Kohlhepp, and P. Marshall, *J. Forensic Sci.*, 2024, **69**, 659-668. https://doi.org/10.1111/1556-4029.15467
7. O. Black, R. Cody, D. Edwards, and J. V. Cizdziel, *Forensic Chem.*, 2017, **5**, 26-32. https://doi.org/10.1016/j.forc.2017.05.003
8. M. Boueri, V. Motto-Ros, W.-Q. Lei, Q.-L. Ma, L.-J. Zheng, H.-P. Zeng, and J. Yu, *Appl. Spectrosc.*, 2011, **65**, 307–314. https://doi.org/10.1366/10-06079
9. D. W. Hahn and N. Omenetto, *Appl. Spectrosc.*, 2012, **66**, 347-419. https://doi.org/10.1366/11-06574
10. M. de Bruin-Hoegée, J. Schoorl, P. Zoon, M. J. van der Schans, D. Noort, and A. C. van Asten, *Forensic Chem.*, 2023, **35**, 100515. https://doi.org/10.1016/j.forc.2023.100515
11. Y. Makonnen and D. Beauchemin, in Sample Introduction Systems in ICPMS and ICPOES, D. Beauchemin, Ed., Elsevier, 2020, 1–55. https://doi.org/10.1016/B978-0-444-59482-2.00001-4
12. A. Ulrich, C. Moor, H. Vonmont, H. R. Jordi, and M. Lory, *Anal. Bioanal. Chem.*, 2004, **378**, 1059-1068. https://doi.org/10.1007/s00216-003-2434-8
13. J. S. Stanberry, H. B. Andrews, C. V. Thompson, B. W. Ticknor, and B. T. Manard, *Anal. Chem.*, 2025, **97**, 1688-1694. https://doi.org/10.1021/acs.analchem.4c04794
14. G. J. Van Berkel, V. Kertesz, and R. C. King, *Anal. Chem.*, 2009, **81**, 7096-7101. https://doi.org/10.1021/ac901098d
15. D. Simon and R. Oleschuk, *Analyst*, 2021, **146**, 6365-6378. https://doi.org/10.1039/d1an00725d
16. M. Trolio, M. Hassan, R. Oleschuk, and D. Beauchemin, *Atom. Spectrosc.*, 2023, **44**, 191-197. https://doi.org/10.46770/AS.2023.101
17. M. Senila, *Sustain. Chem.*, 2026, **7**, 28. https://doi.org/10.3390/suschem7030028